Cohesive Contact Modeling in Thermoforming Simulations of Metal-CRFP-Metal Sandwich Sheets

Özgür Cebeci [1], Malte von Scheven [2], Andreas Zeiser [1]

[1] Inpro Innovationsgesellschaft für fortgeschrittene Produktionssystem in der Fahrzeugindustrie mbH, Berlin, Deutschland

[2] Institut für Baustatik und Baudynamik, Universität Stuttgart, Stuttgart, Deutschland

Abstract

A novel carbon fiber reinforced metal laminate based on thermoplastic polymer is investigated in the project LEIKA. For the safeguarding of the production of the parts made of this material, coupled thermo-mechanical simulations have to be carried out. Experiments show a large relative sliding, separation and re-sticking behavior between layers during the forming of the heated sheets. Hence, each layer of the laminate needs to be modeled as an individual shell in order to represent the different forming behavior.

In this work we concentrate on the complex interlayer contact behavior. As the built-in contact models in LS-DYNA are not capable of modeling all relevant physical aspects, a new temperature dependent traction-separation model has been developed based on a bi-functional cohesive definition with damage (RCCM). For the post separation state the model has been extended with a pressure dependent re-sticking and adhesive re-healing. For the tangential behavior either a temperature dependent Coulomb friction or a hydrodynamic friction law can be used. The model has been implemented into LS-DYNA using the user-defined friction routine. It has been verified and applied the deep drawing of test parts. For the latter case the simulation results show good agreement with experimental results provided by partners.

Keywords: Thermoforming, CFRP, Finite Elements, Cohesive Contact, LS-DYNA

1 Introduction

Weight reduction is essential for the development of new vehicles especially in the case of electric cars [1]. In turn it allows the down-sizing of the cost intensive battery system leading to economic benefits. Function-integrative lightweight engineering in multi-material-design is the most promising approach to tap the full potential. In this strategy, new innovative material combinations play an important role [2]. In this regard sandwich materials allow to combine the advantages of different materials. In the interdisciplinary research project LEIKA a novel laminate combining carbon fiber-reinforced thermoplastic and metal is investigated (see figure 1). The aim of the project is to set up a development and manufacturing chain for metal-CFRP laminates and parts made of this material. In the forming step for producing parts, the semi finished sheets are heated and subsequently formed in a stamping process. For the commercial application of the material a virtual safeguarding of this process is a necessity.

Due to the different forming behavior of the materials, experiments show a large relative sliding, separation and re-sticking behavior between layers during the forming of the heated sheets. Therefore, using an individual shell mesh for each layer this behavior can be represented in the simulation (see figure 2). In this regard, interlayer contact modeling becomes significantly important. As a result of the melt polymer continuum at the high forming temperatures, a particular care has to be taken for the interlayer contact modeling.

In this work we concentrate on the complex interlayer contact behavior. For the modeling of the cohesive interlayer behavior the main idea is to apply traction separation laws in the normal direction and use friction laws for the tangential force components.
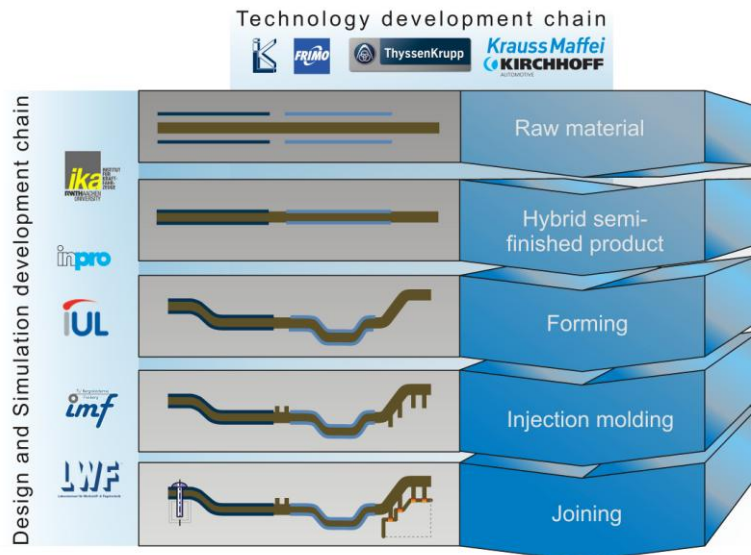
Fig 1: LEIKA project chain

The only available built-in contact model in LS-DYNA which allows tangential movement and constrains the normal separation is ***Contact_Surface_to_Surface_Tiebreak** with the separation option 4 [3]. It applies a linearly increasing reaction force in the normal direction with an instantaneous failure. Also re-sticking cannot be represented by this model.
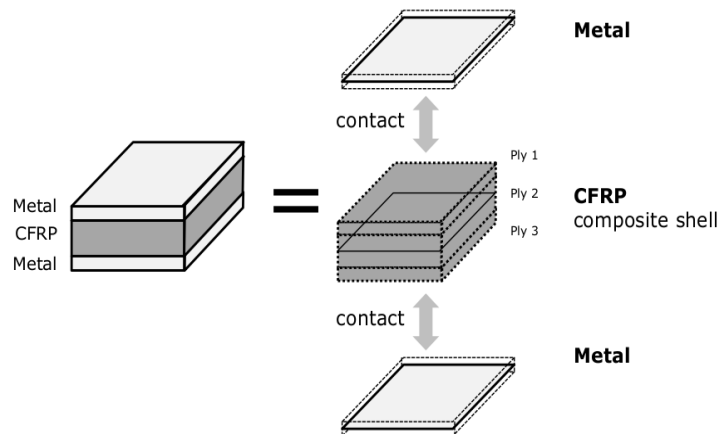

Fig 2: Three layer shell approach

Since the built-in contact models in LS-DYNA are not capable of modeling all the relevant physical aspects, an improved user defined contact model has been developed and implemented using the LS-DYNA user defined friction routine. The main goal of the developments is to provide a smooth traction separation behavior with damage and re-sticking properties.

2 Experimental Studies

In order to investigate the formability of the corresponding sandwich structures, several forming tests have been carried out in LEIKA project. In particular bending and drawing based tests have been designed in order to represent distinct deformation modes that often occurs in the forming of metal sheets.

Initial tests confirm that, in the case of drawing, larger interlayer sliding as well as interlayer separation and damage come into play. In those experiments, void formations have been observed during the forming process. In this regard it has been found necessary to carry out further studies on separation and damage characteristic of the interlayer continuum.

2.1   Separation behavior of soft adhesive bonds

An experimental setup for the investigation of soft adhesive bonds, so called probe test, is given in [4]. Probe test consists of a transparent rigid surface which is bonded with a metal probe by a soft adhesive layer. Bonding can be either provided initially or probe can get in touch and stick to the soft polymer continuum. Therefore both scenarios have been considered during the experiments. The main idea of the experiment is to capture the evolution of damage during the debonding.

In this framework, corresponding test is given for a soft acrylic adhesive layer with the thickness of 0.1mm. Results have shown that, loading leads void grow and consequently damage develops in the soft polymer continuum as it can be seen in the firgure 3.

Taking into account the given similarities between soft adhesives and the polymer melts along with the similar failure mechanism, for the further numerical applications the values given in the figure 3 are taken as the reference for interlayer contact behavior.
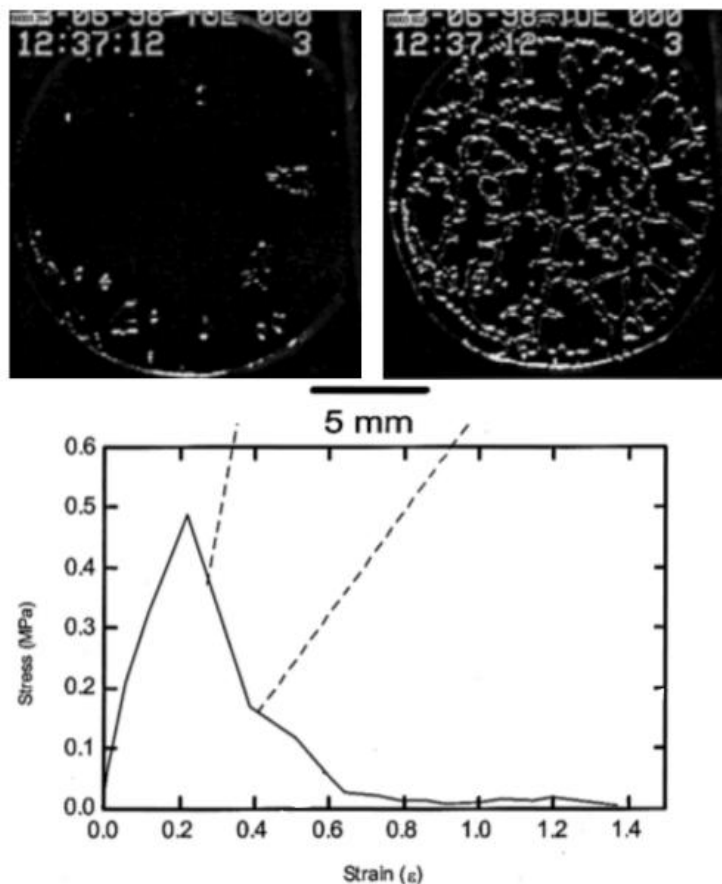

Fig 3: Probe test results [4]

A linear increase and subsequently decay (as a result of the damage) of the separation force can be seen in figure 3. For the modeling of such a behavior, RCCM model given by [5] is investigated.

3 Investigation of the bi-functional traction separation law (RCCM model)

A bi-functional traction separation law is described in the framework of damage mechanics by [5] modeling a certain decay in the interface stiffness with respect to increasing loading. Model have been developed based on the description of the contact interface considering the material theories. Therefore, corresponding free energy function and dissipation potential are derived and thermodynamical consistency of the model is proved with CLAUSIUS-DUHEM inequality. Additionally, the reader can find the details about the variational existence and uniqueness of the problem in the corresponding paper.

The model uses an evolution function for the adhesive intensity β in order to govern the adhesive decay. In this regard the corresponding constitute law is given for normal contact respectively in equation 1 and equation 3 where p_N is the normal contact stress, C_N is the normal contact stiffness and g_N stands for the separation distance.

$$-p_N + C_N g_N \beta^2 \geq 0, \quad g_N \geq 0, \quad (-p_N + C_N g_N \beta^2) g_N = 0 \quad (1)$$

$$\beta : \begin{cases} 1, & \text{total adhesion} \\ 0 < \beta < 1, & \text{partial adhesion} \\ 0, & \text{no adhesion} \end{cases} \quad (2)$$

The governing differential equation for the adhesive evolution along with the evolution condition can be seen in equation 3.

$$\dot{\beta} = \begin{cases} [\frac{1}{\eta}(\omega \frac{\partial h(\beta)}{\partial \beta} - (C_N g_N^2)\beta)]^{\frac{1}{\rho}}, & \omega \frac{\partial h(\beta)}{\partial \beta} \leq (C_N g_N^2)\beta \\ 0, & \omega \frac{\partial h(\beta)}{\partial \beta} > (C_N g_N^2)\beta \end{cases} \quad (3)$$

Taking a detailed look at the governing function, it can be seen that η governs the rate dependencies and $\partial h(\beta)/\partial \beta$ and ρ are the adjustment terms.

Validation of the given model has been carried out with respected to the experimental results from section 2. In this regard, respectivelly the effects of the viscous parameter η and the separation rate can be seen in the following figures.
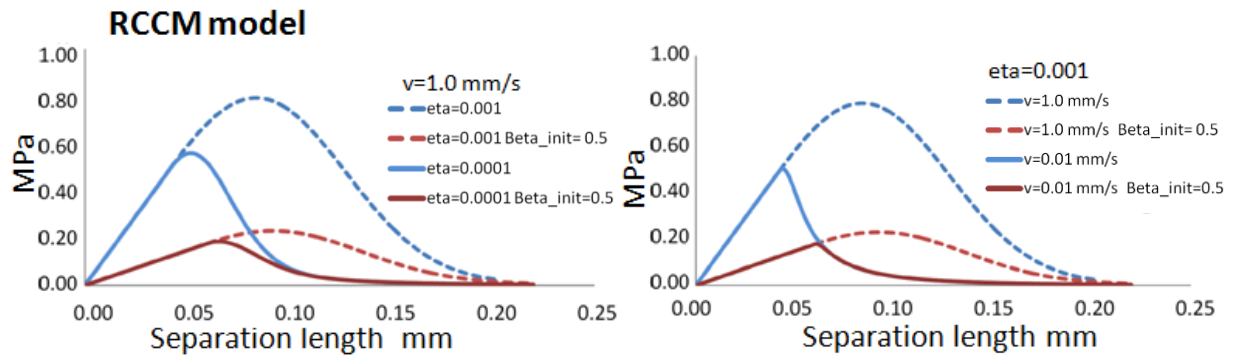

Fig 4: Validation of the RCCM model. Left, effect of the viscous parameter; right, effect of the separation rate

3.1   Adhesive re-healing

Re-sticking is an observed phenomena for polymer melts and soft polymers. In this regard, idea of the reversible damage or adhesive intensity is represented in a thermodynamical framework in [6]. Also the variational existence of the adhesive re-healing has been discussed by the same authors in [7]. In this regard, we introduce a pressure dependent recovery function (see equation 4) where ζ is the recovery parameter.

$$\beta^{rec} = \int_0^t (\zeta P(t)_N^+) \, d\tau \quad (4)$$

Re-healing factor ζ can be defined by considering a complete damage recovery under a certain pressure and time range. Here it needs to be noted that, yet there is no literature regarding to the thermodynamics of adhesive re-healing procedure. Therefore, the re-healing function has been introduced based on the intuitions gathered from observations. Further studies should be carried out in order to proof the thermodynamical consistency of the introduced function.

4 Numerical Implementations

The models described in the last section have been implemented using the user-defined friction subroutine in LS-DYNA. At this point, the main approach is to scale the master segment thickness in order to provide an extra zone for cohesive separation. However as LS-DYNA also computes the reaction forces for this zone, the normal forces have to be corrected.

The user-defined friction routine allows the user to access all state variables and model parameters needed for computation. This includes the master segment normal vector, the slave node area, the projected slave node coordinates, the penalty factor, the time step size, the incremental displacement vectors and the nodal temperatures. Additionally, the routine uses the history variable array to store state values for active slave node set.

The control parameters are provided by "user-array" in input deck. In this way different flags and constitutive parameters can be defined in the standard LS-DYNA input format.

4.1 Algorithmic structure

In LS-DYNA the user defined friction routine is called for each time step for the active node set . In our implementation the contact forces are calculated according to the model described in Section 3 for each slave node.

First the penetration distance is calculated depending on the segment types and the scaled master segment thickness. At this point the compensation of the forces are computed with respect to the corresponding penetration depth and the penalty factor. Normally damping forces are computed automatically for each slave node. However this also includes approaching nodes which have not been in contact yet. To elememinate the damping for these nodes the standard damping forces are disabled in standard contact card. For the other slave nodes the damping is computed in the user defined routine according to [8].

The frictional forces are computed using the default routine. Alternatively, hydrodynamic friction law with temperature dependent behavior has been implemented and can be used.

The core of the implementation is the distinct treatment of the approaching, normal penetration and the separation states by using the history variables. For the approaching case, as there is no contact all slave node forces are set to zero. Later, for the contact penetration, forces are computed with respect to standard penalty method and the compensation forces are applied along with friction and damping force components. In the contact penetration case, as it is given in equation 5, pressure dependent incremental recovery routine is called. Furthermore the recovery characteristic can also be defined temperature dependent.

$$\Delta \beta_{n+1}^{rec} = \begin{cases} 0, & P_N < 0 \quad \text{and} \quad \beta = 1 \\ \zeta P_{n+1} \Delta t, & P_N \geq 0 \quad \text{and} \quad 0 < \beta < 1 \end{cases} \qquad (5)$$

For the separation state, cohesive forces are computed with respect to the elastic energy limit ω which depends on the prescribed ultimate normal separation stress (see equation 6).

$$\omega = \sigma_{max}^2 / C_N \qquad (6)$$

Considering the high frequency vibrations and dynamic nature of the explicit analysis, backward Euler scheme has been used for the solution of the evaluation function. Defining ∂h(β) /∂β and ρ as unit, the solution is given in equation 7.

$$\beta_{n+1} = (1 - \frac{\Delta t_{n+1}}{\eta}(C_N g_N^2))^{-1}(\beta_n - \frac{\Delta t_{n+1}}{\eta}\omega) \qquad (7)$$

Subsequently the adhesive intensity can be written with respect to the re-healing contribution (see equation 8).

$$\beta_{n+1} = \beta_{n+1} + \Delta \beta_{n+1}^{rec}) \qquad)$$

At the end the normal separation stress can be given as following, where adhesive intensity β is stored as a history variable.

$$p_{Nn+1} = C_N g_{Nn+1} \beta_{n+1}^2 \quad (9)$$

4.2 Temperature dependency

The idea for the temperature dependencies is to define parameters for two different temperature regions and use a smooth cubic transition function for the transient region. For each constitutive parameter, control arguments can be defined using the "user-array". In above given framework maximum separation stress, re-healing factor and friction behavior can be controlled depending on the slave segment temperature.

5 Numerical Applications

In this part numerical applications of the developed contact model are given where implementations have been tested in a systematic way with different models.

In all simulations, the developed contact model has been used together with ***Contact_one_way_surface_to_surface** definition. The contact implementation uses standard contact penalty as given by LS-DYNA. Therefore the standard critical time step calculations can be applied.

5.1 Fundamental model

In order to test the developments without any other complication a basic model consisting of two shell bodies has been used (see figure 5). The bottom part is defined as the master segment and it is constrained in all degrees of freedoms. The upper part is defined as slave segment and subjected to prescribed displacement. The upper part moves downward and upwards in order to represent the penetration-separation sequences. Additionally it has been subjected to constant tangential velocity.
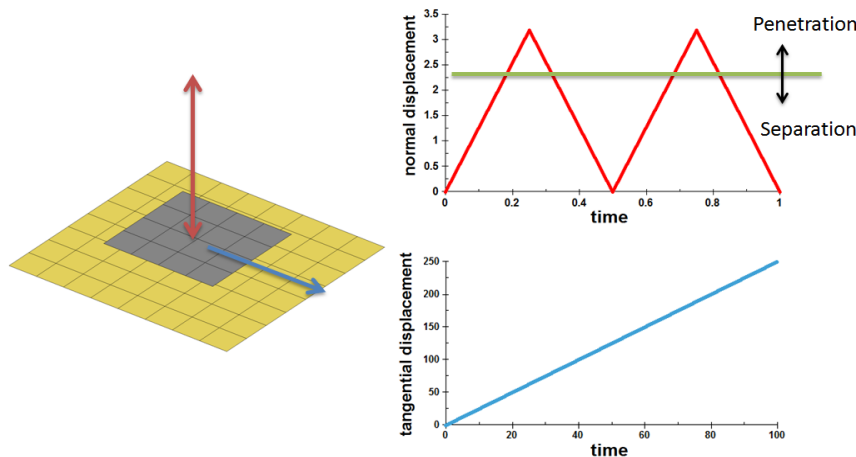

Fig 5: Fundamental model

RCCM model has been tested and as it can be seen in the figure 6, during the penetration, classical penalty and friction forces apply. Later as it has been expected, in the separation state normal force increases linearly and smoothly decays beyond the elastic energy limit.
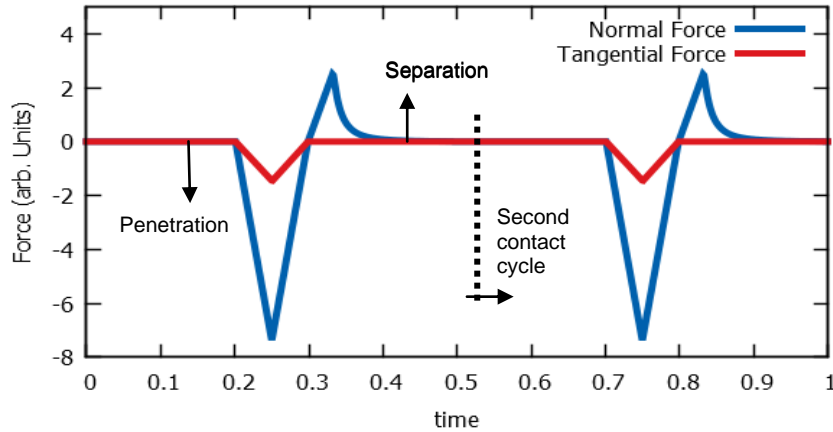
Fig 6: Fundamental, contact forces vs. time

Also together with the adhesive re-healing, re-sticking behaviour can be observed in second contact cycle.

In order to observe the softening behavior as a result of the adhesive evolution, a slightly different normal displacement is applied to the fundamental model. The separation is limited such that only partial damage but no complete failure occurs. The evolution of damage can be observed in figure 7.
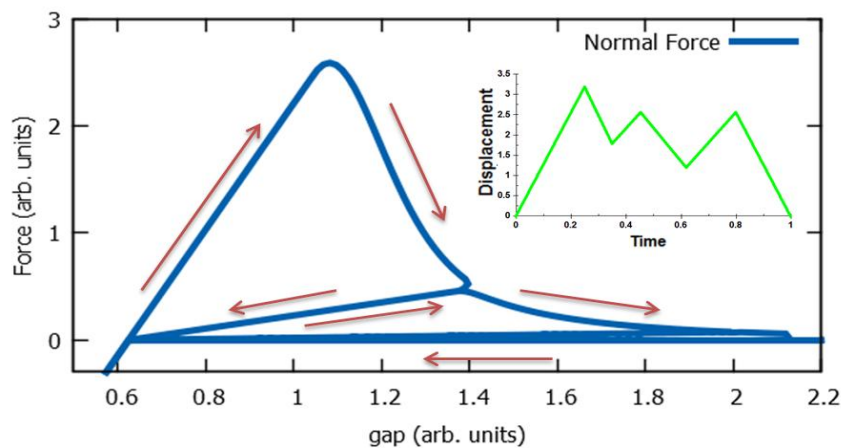

Fig 7: Damage behavior

5.2   Deformable test model

As the next step, the developed contact model has been applied to a deformable body. As it can be seen in figure 8, a solid domain has been discretized with smaller element size on the contact surface in order to get a smoother separation behaviour. For the discretization, standard 8 node solid elements are used. In order to provide a compete assessment for the performances of the developed contact model, the deformable solid body has been designed as a soft hyperelastic continuum that can be subjected to finite strains. In this framework, Mooney-Rivlin rubber is chosen as the material model with the elastic constants of 0.2 MPa and poisons ratio as 0.49. In the corresponding simulations maximum separation stress has been defined as 0.3 MPa.
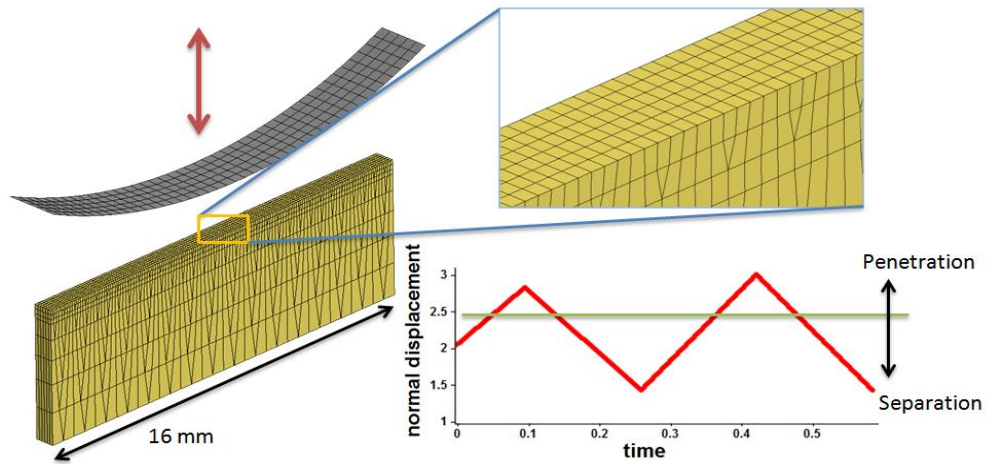
Fig 8: Deformable test model

A pressure fringe plot for the RCCM model is provided in figure 9. As it is given, during the movement of the cylindirical tool, pressure increases and with the separation, negative stresses can be seen along with the corresponding deformation.

Figure 10 (right) shows the interface pressure results at two different interface location. The maximum separation stresses are consistent with the defined value of 0.3 MPa. Additionally, in order to interpret the different separation responses for the two different spots that occur during the simulation, the adhesive intensities also have to be taken into account, which are displayed in figure 10 (left).
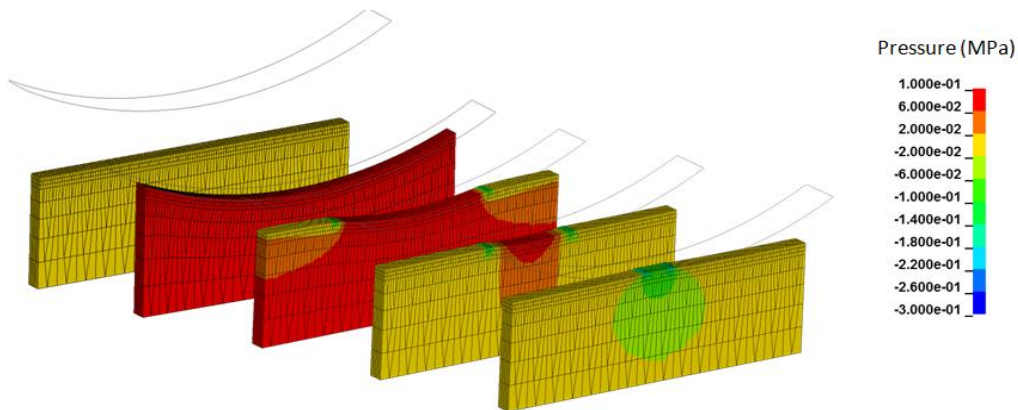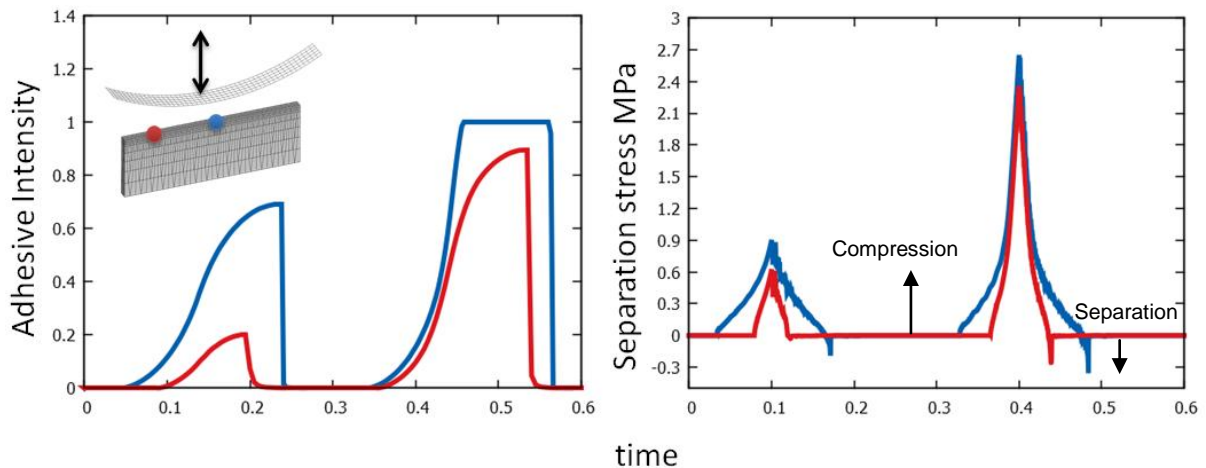

Fig 9: RCCM model pressure fringe results

Fig 10: Results from two different locations. Left, adhesive intensity; Right, separation pressure

5.3 Deep drawing

Finally, the development has been tested with the real parts. As it involves lateral contact, friction and cohesive separation conditions at the same time, deep drawing is a challenging case study for the developed contact model.

In the drawing experiments a three layered semi-finished carbon fibre sandwich sheet has been used. The work piece consists of metal and woven composite layers with 0.25 mm and 1.00 mm thickness.
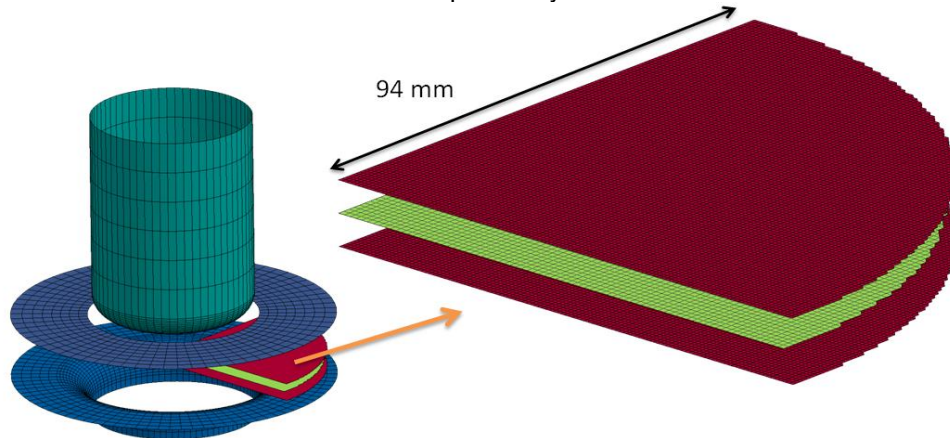

Fig 11: Deep-drawing model with three layer shell approach

Simulations have been carried out by modelling each layer with shell elements, as it is given in figure 11. In this regard the developed contact model has been used for interlayer contact modelling by choosing the middle layer as master and outer layers as slave segments. For the rest of the contact couplings, built-in contact models in LS-DYNA have been used. Because of the master-slave segment choice in the work piece, for the middle layer slightly larger discretization have been preferred.
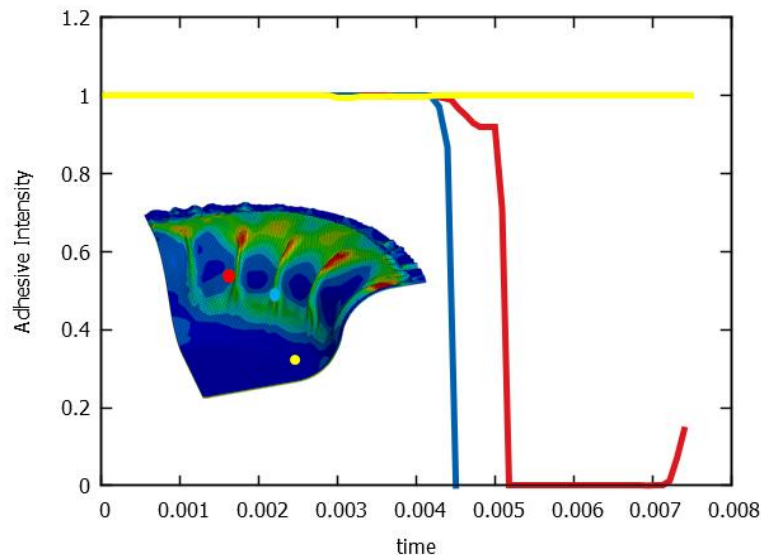

Fig 12: Result of the deep drawing simulations, plastic strain contour and evaluation of the adhesive intensity from 3 different locations

The result of the corresponding simulation can be seen in figure 12 where plastic strain and adhesive intensities are depicted. As the given figure shows, during the process large interlayer sliding and wrinkling can be observed. As it can be seen from the adhesive intensity results, the wrinkling zone subjected to adhesive decay and subsequently re-healing. On the other hand, adhesive intensity stays constant in the wrinkle free zone as expected.
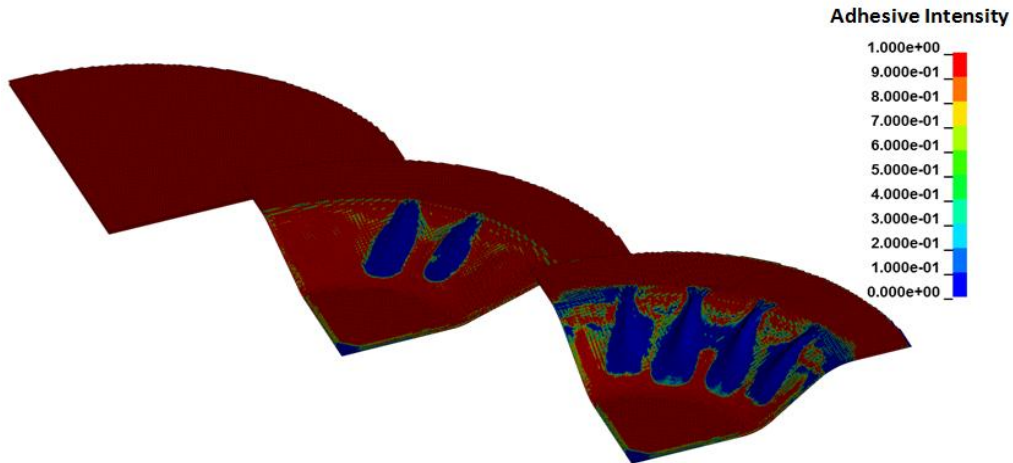
Fig 13: Adhesive intensity contour

For a refined model the adhesive intensity parametner β is displayed in figure 13 using LS-PrePost.

Fig 14: Comparison of the deep-drawing results [9]

Lastly, using the Hyperview as post-processing tool, a full image of the symmetric model has been created. The corresponding results are compared with experimental results obtained by IUL at University of Dortmund [9] in figure 14. As it can be seen, regarding the deformation patterns results are in a good agreement. However, it has to be noted that described simulation model ends up with some stability issues. Therefore, further studies have be carried out on these stability problems.

6 Summary and outlook

In the scope of this work a new contact model for thermoforming simulations of metal carbon semi-finished sandwich sheets has been developed. The model has been implemented in LS-DYNA using the user-defined friction routine. The simulation results are in a qualitative agreement with the experiments.

At this point, considering the complexity of the corresponding drawing simulation, performance of the model can be regarded fairly promising. For the sake of robustness of such simulations, the observed in stabilities should be identified and eliminated. However in such complex models, it is not always

easy to distinguish the source of the instabilities. For improving the contact modeling the two-way contact algorithms are expected to improve stability. On the theoretical side the thermodynamical consistency of the model should be investigated.

7 Literature

[1] Eckstein L., Hartmann B., Schmitt F., "Leichtbau bei Elektrofahrzeugen", Automobiltechnische Zeitschrift 11/2010.

[2] Hufenbach W., Adam F., Krahl M., Geller S., "Ganzheitliche Lösungsstrategien bei der Entwicklung von Faserverbundkomponenten für automobile Leichtbauanwendungen", Proceedings of the 2nd International Conference on Advanced Metal Forming Processes in Automotive Industry AutoMetForm 2010, Freiberg, Germany, pp. 58-69.

[3] Livermore Software Technology Corporation, "LS-DYNA Keyword Manual Vol I" - Contact, retrieved February 16, 2015, http://lstc.com/download/manuals

[4] Creton C., Hooker J., "Bulk and Interfacial Contributions to the Debonding Mechanisms of Soft Adhesives: Extension to Large Strains", Langmuir, 17, 2001, 4948-4954

[5] Raous M., Cangemi L., Cocu M., "A Consistent Model Coupling Adhesion, Friction, and Unilateral Contact", Computational Methods Applied Mechanics and Engineering, 177, 1999, 383-399

[6] Raous M., Schryve M., Cocou M., "Recoverable adhesion and friction", in "Proceedings of the Second International Conference on Nonsmooth/Nonconvex Mechanics with Applications in Engineering, Thessaloniki, Greece, July 7-8, 2006" C.C. Baniotopoulos (ed.), Editions Ziti, pp. 165-172, 2006.

[7] Cocou M., Schryve M., Raous M., "A dynamic unilateral contact problem with adhesion and friction in viscoelasticity", Z. Angew. Math. Phys., 61, 2010, 721–743.

[8] Livermore Software Technology Corporation, "LS-DYNA Theory Manual"-Contact, retrieved January 29, 2015, http://lstc.com/download/manuals

[9] Tekkaya A. E., Hahn M., Hiegemann L., Weddeling C., Ben Khalifa N., "Umformen faserverstärkter thermoplastischer Kunststoff-Halbzeuge mit metallischen Deckblechen für den Leichtbau", Proceedings of 35. EFB-Kolloquium Blechbearbeitung 2015, 24./25. March 2015, Bad Boll, 185-199